Agricultural and Biosystems Engineering Publications

Agricultural and Biosystems Engineering

2005

Modeling Sediment Trapping in a Vegetative Filter Accounting for Converging Overland Flow

Matthew J. Helmers
Iowa State University, mhelmers@iastate.edu

Dean E. Eisenhauer
University of Nebraska–Lincoln

Thomas G. Franti
University of Nebraska–Lincoln

Michael G. Dosskey
United States Department of Agriculture

Modeling Sediment Trapping in a Vegetative Filter Accounting for Converging Overland Flow

Abstract

Vegetative filters (VF) are used to remove sediment and other pollutants from overland flow. When modeling the hydrology of VF, it is often assumed that overland flow is planar, but our research indicates that it can be two-dimensional with converging and diverging pathways. Our hypothesis is that flow convergence will negatively influence the sediment trapping capability of VF. The objectives were to develop a two-dimensional modeling approach for estimating sediment trapping in VF and to investigate the impact of converging overland flow on sediment trapping by VF. In this study, the performance of a VF that has field-scale flow path lengths with uncontrolled flow direction was quantified using field experiments and hydrologic modeling. Simulations of water flow processes were performed using the physically based, distributed model MIKE SHE. A modeling approach that predicts sediment trapping and accounts for converging and diverging flow was developed based on the University of Kentucky sediment filtration model. The results revealed that as flow convergence increases, filter performance decreases, and the impacts are greater at higher flow rates and shorter filter lengths. Convergence that occurs in the contributing field (in-field) upstream of the buffer had a slightly greater impact than convergence that occurred in the filter (in-filter). An area-based convergence ratio was defined that relates the actual flow area in a VF to the theoretical flow area without flow convergence. When the convergence ratio was 0.70, in-filter convergence caused the sediment trapping efficiency to be reduced from 80% for the planar flow condition to 64% for the converging flow condition. When an equivalent convergence occurred in-field, the sediment trapping efficiency was reduced to 57%. Thus, not only is convergence important but the location where convergence occurs can also be important.

Keywords

Flow convergence, Grass filters, Hydrologic modeling, Overland flow, Sediment trapping, Two-dimensional overland flow, Vegetative filters

Disciplines

Agriculture | Bioresource and Agricultural Engineering

Comments

MODELING SEDIMENT TRAPPING IN A VEGETATIVE FILTER ACCOUNTING FOR CONVERGING OVERLAND FLOW

M. J. Helmers, D. E. Eisenhauer, T. G. Franti, M. G. Dosskey

ABSTRACT. *Vegetative filters (VF) are used to remove sediment and other pollutants from overland flow. When modeling the hydrology of VF, it is often assumed that overland flow is planar, but our research indicates that it can be two-dimensional with converging and diverging pathways. Our hypothesis is that flow convergence will negatively influence the sediment trapping capability of VF. The objectives were to develop a two-dimensional modeling approach for estimating sediment trapping in VF and to investigate the impact of converging overland flow on sediment trapping by VF. In this study, the performance of a VF that has field-scale flow path lengths with uncontrolled flow direction was quantified using field experiments and hydrologic modeling. Simulations of water flow processes were performed using the physically based, distributed model MIKE SHE. A modeling approach that predicts sediment trapping and accounts for converging and diverging flow was developed based on the University of Kentucky sediment filtration model. The results revealed that as flow convergence increases, filter performance decreases, and the impacts are greater at higher flow rates and shorter filter lengths. Convergence that occurs in the contributing field (in-field) upstream of the buffer had a slightly greater impact than convergence that occurred in the filter (in-filter). An area-based convergence ratio was defined that relates the actual flow area in a VF to the theoretical flow area without flow convergence. When the convergence ratio was 0.70, in-filter convergence caused the sediment trapping efficiency to be reduced from 80% for the planar flow condition to 64% for the converging flow condition. When an equivalent convergence occurred in-field, the sediment trapping efficiency was reduced to 57%. Thus, not only is convergence important but the location where convergence occurs can also be important.*

Keywords. *Flow convergence, Grass filters, Hydrologic modeling, Overland flow, Sediment trapping, Two-dimensional overland flow, Vegetative filters.*

Vegetative filters (VF) are used to control sediment delivery to water bodies. VF retard flow velocity and reduce the transport capacity of water flow (Tollner et al., 1982). As a result, some of the sediment will be deposited as water flows through the VF. While there has been a significant amount of research performed on plot-scale VF and on laboratory-scale filters using either real vegetation or simulated vegetation, very little information is available on water flow and sediment transport within field-scale VF (Daniels and Gilliam, 1996; Dillaha et al., 1989, Munoz-Carpena et al., 1999; Schmitt et al., 1999; Sheridan et al., 1999). In this article, field scale differs from plot scale in that the flow lengths within the filter and the loading of water and sediment to the filter are representative of field conditions, and flow pathways are not controlled by artificial plot borders.

Current models of overland flow and sediment movement through VF only apply to one-dimensional or uniformly distributed flow (i.e., planar). REMM (Lowrance et al., 2000) and VFSMOD (Munoz-Carpena et al., 1999), which are models that simulate processes that occur in VF, use this assumption. Overland flow within a VF that was investigated during this study was found to be two-dimensional with converging and diverging pathways (Helmers, 2003). Dillaha et al. (1989) stated that VF that are characterized by concentrated flow should be less effective for sediment removal than filters with shallow, uniformly distributed flow. However, there is little quantitative information on the impact of convergence of overland flow on sediment trapping in a VF. Our hypothesis is that flow convergence will negatively influence the sediment trapping capability of VF. The objectives of this investigation were: (1) to develop a modeling approach for estimating sediment trapping in a VF that accounts for converging or diverging flow, and (2) to use this model to investigate the impact of converging overland flow on sediment trapping within a VF.

MODELING

To model sediment trapping in a VF, infiltration and overland runoff must be modeled along with modeling of sediment trapping in the VF. The hydrologic processes were modeled using MIKE SHE (Refsgaard and Storm, 1995)

The authors are **Matthew Justin Helmers, ASAE Member,** Assistant Professor, Department of Agricultural and Biosystems Engineering, Iowa State University, Ames, Iowa; **Dean E. Eisenhauer, ASAE Member,** Professor, and **Thomas G. Franti, ASAE Member,** Associate Professor, Department of Biological Systems Engineering, University of Nebraska-Lincoln, Lincoln, Nebraska; and **Michael G. Dosskey,** Research Ecologist, USDA National Agroforestry Center, University of Nebraska, Lincoln, Nebraska. **Corresponding author:** M. J. Helmers, Department of Agricultural and Biosystems Engineering, Iowa State University, Ames, Iowa 50011; phone: 515-294-6717; fax: 515-294-2552; e-mail: mhelmers@iastate.edu.

following the procedures outlined by Helmers (2003). Sediment trapping was modeled using a modeling approach based on the University of Kentucky sediment filtration model. MIKE SHE is a deterministic, distributed and physically based model that allows for simulation of all major hydrological processes occurring in the land phase of the hydrologic cycle (Refsgaard and Storm, 1995). MIKE SHE solves the equations of continuity and conservation of momentum in two horizontal directions to describe the overland flow process. The conservation of momentum equations are solved using the diffusive wave approximation. The Strickler/Manning-type law is used for the friction slope with a Strickler roughness coefficient input at each computational location (Refsgaard and Storm, 1995). Infiltration is described using one-dimensional vertical flow by solving Richards' equation (Kutilek and Nielson, 1994).

UNIVERSITY OF KENTUCKY SEDIMENT FILTRATION MODEL

The University of Kentucky sediment filtration model used in this study considers sediment type and concentration, flow conditions, vegetation conditions, and filter length (Barfield et al., 1979; Hayes et al., 1979, 1984; Tollner et al., 1976, 1977, 1982). Equations and nomenclature used in the University of Kentucky sediment filtration model are provided in the Appendix in tables A.1 and A.2, respectively.

The bed shear in the channel is described using the channel slope and the hydraulic radius, based on the spacing of media elements and flow depth (eqs. A.1 and A.2). Flow hydraulics in the vegetation are represented by a calibrated form of the Manning equation and the principle of continuity (eqs. A.3 and A.4). Haan et al. (1994) give values for the calibrated Manning's roughness coefficient ranging from 0.037 to 0.074. Tollner et al. (1982) analyzed the suitability of Einstein's (1942) sediment transport relationships to predict sediment transport in a simulated rigid media using the bed shear from equation A.1 (eqs. A.5, A.6, A.7, A.8, and A.9).

The University of Kentucky sediment filtration model considers sediment transport and deposition in four zones of a vegetative filter, A(t), B(t), C(t), and D(t), as shown in figure 1. In general, the trapping in zones A(t) through C(t) is referred to as depositional wedge trapping, and zone D(t) is considered the suspended load trapping zone. It is assumed that the only material deposited in the upstream delta and in zones A(t) to C(t) are coarse particles larger than 0.037 mm. The fraction of the sediment trapped in the wedge is found by continuity using equation A.10, and the average sediment load on the depositional wedge can be defined from equation A.11.

For zone D(t), it is assumed there has been insufficient deposition on the bed to allow bed load transport; thus all the sediment reaching the bed is trapped. Tollner et al. (1976) proposed that the probability of sediment trapping is related to the potential number of times a particle could fall from the water surface to the bottom of the channel (eqs. A.12, A.13, and A.14). The assumption that all particles reaching the bed are trapped becomes questionable with time and deposition. Based on this, Wilson et al. (1982) proposed a correction function to the trapping efficiency in zone D(t) (eqs. A.15 and A.16).

Sediment transport through the VF is divided into three classes. The three classes and particle size breakdown are:

Coarse: $d_p > 0.037$ mm

Medium: 0.004 mm $< d_p < 0.037$ mm

Fine: $d_p < 0.004$ mm.

Haan et al. (1994), based on observations by Hayes et al. (1984), stated that it was apparent that particles smaller than 0.037 mm were not trapped in the wedge, and particles smaller than 0.004 mm were not trapped by settling in zone D(t). Thus, only the coarse particles are considered in calculating the trapping in the depositional wedge, and all three classes are considered in calculating the trapping in zone D(t). Inamdar (1993) stated that particles smaller than 0.004 mm in diameter are not expected to be trapped due to settling.

Hayes et al. (1984) evaluated the impact of infiltration on sediment deposition in zone D(t) by assuming that the difference in flow rate between the inlet and outlet of the filter is only a result of infiltration, and that the mass of sediment in a given infiltration volume is either transported into the soil matrix or trapped on the soil surface. Haan et al. (1994) presented a dimensionless term (I) that is related to the average infiltration rate and used to account for infiltration in the trapping in zone D(t) (eqs. A.17 and A.18).

The discussion of the University of Kentucky sediment filtration model to this point considers zone D(t) to be one unit. However, Inamdar (1993) presents a modification to equation A.12 in which the filter length is divided into a number of segments and the total trapping in the filter is determined by summing the trapping efficiencies of the individual segments. The modification factor was used in modeling sediment trapping in a VF considering channelization of flow where channelization varied throughout the filter and a segmental approach was needed. The channel network in Inamdar's study was represented stochastically. The trapping of an individual segment is computed using equations A.19 and A.20. By transmitting the outflow of
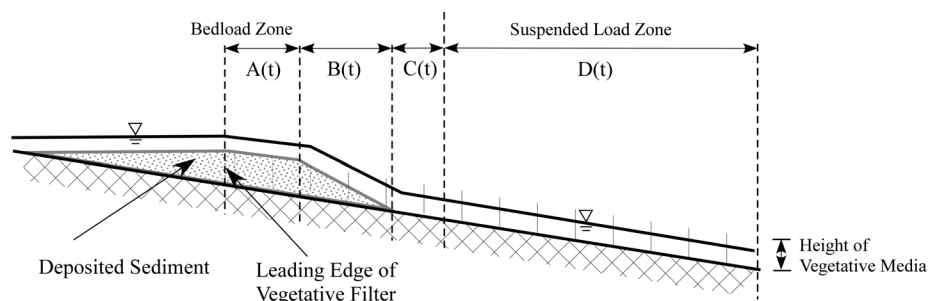

Figure 1. Schematic of University of Kentucky sediment filtration model (modified from Hayes et al., 1984).
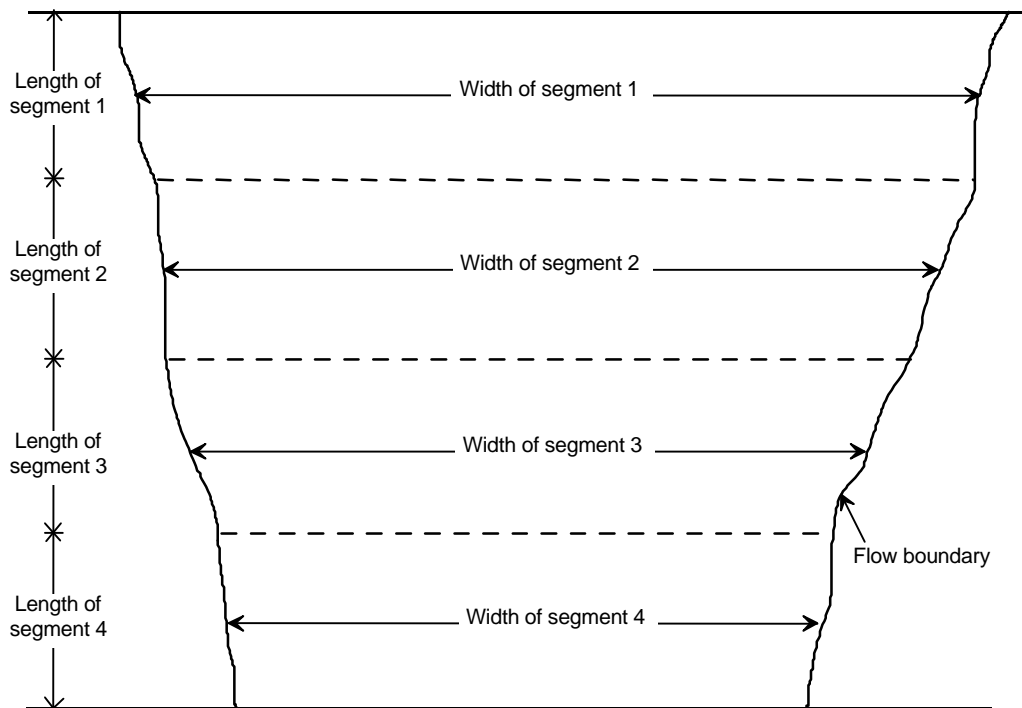
Figure 2. Segmental approach to sediment trapping in a vegetative filter. Note that segmental width varies through the filter depending on overland flow pathways, but segmental width is constant.

sediment from one segment to the next and applying the segmental trapping to determine the outflow of sediment to the next segment, the total trapping of the filter can be computed.

SEDIMENT FILTRATION MODEL

To analyze converging and diverging flow areas, the University of Kentucky sediment filtration model was programmed in a spreadsheet for use in computing sediment filtration in a VF using the segmental approach presented by Inamdar (1993). Using the segmental approach allows the width over which the overland flow is distributed to vary so that converging and diverging flow areas can be modeled (i.e., the length of each segment is constant, but the width of the segment may vary) (fig. 2). It is assumed that flow is uniformly distributed over the width of the segment. A flowchart for the spreadsheet program is provided in figure 3. The input parameters are noted in the flowchart, as are the equations used to perform the computations in each segment of the filter. To account for cases where the sediment transport capacity decreases due to diverging flow or infiltration, the sediment mass flow rate is compared to the sediment transport capacity in each segment to account for deposition by this mechanism. In the spreadsheet program, the depositional profile of the wedge is not computed, but the sediment deposition in zone D is computed to allow for use of the depth correction factor reported by Haan et al. (1994) from Wilson et al. (1982).

To compute the fraction of sediment trapped, the unit flow rate, sediment concentration, and sediment characteristics including the fraction larger than 0.037 mm must be known. The output from MIKE SHE was used in the spreadsheet model as the hydrologic input in each segment of the VF. From the coarse fraction and a particle size distribution curve, the mean particle size of the coarse fraction is computed for use in calculating the sediment transport

capacity. The mean particle size used in computation of the sediment transport capacity of the coarse fraction is the particle size at the midpoint between the fraction finer than 0.037 mm and 1. The fraction of sediment finer than 0.037 mm entering zone D is computed by:

$$D_{37} = \frac{1 - C_{f37}}{1 - f\, C_{f37}} \qquad (1)$$

where D_{37} is the fraction of sediment finer than 0.037 mm after depositional wedge trapping, C_{f37} is the coarse fraction of sediment at the entrance to the filter, and f is the fraction of incoming coarse sediment deposited in the depositional wedge.

The average fraction finer for the coarse material is computed by:

$$D_{ACW} = \frac{1 + D_{37}}{2} \qquad (2)$$

where D_{ACW} is the average fraction finer for the coarse material after wedge deposition.

The average fraction finer for the coarse material after wedge deposition is converted to the fraction finer on the original particle size distribution curve corresponding to the same particle size. The fraction finer on the original curve is computed by:

$$D_{OCW} = D_{ACW}(1 - f\, C_{f37}) \qquad (3)$$

where D_{OCW} is the fraction finer on the original particle size distribution curve corresponding to fraction finer of coarse material after wedge deposition. The D_{OCW} value is used to estimate the mean particle size of the coarse fraction entering zone D.

Soil Inputs

| Average sediment concentration and particle size distribution |

Variable Inputs

| Segment width |

| Hydrologic input – Hydrograph (flow rate per unit width) (L/m/s) |

Segment 1

Compute sediment trapping with University of Kentucky model (Equations A.2, A.3, A.5, A.7, A.9, A.10, A.15, A.16, A.18, A.19, and A.20)

Constant Inputs

| Slope, calibrated Manning's roughness, porosity, grass spacing, particle density, segment length, and number of segments |

Outflow of sediment from segment 1 (mass loading)
Inflow of sediment to segment 2 (mass loading)

| Segment width |

| Hydrologic input – Hydrograph (flow rate per unit width) (L/m/s) |

Segment 2

Compute sediment trapping with University of Kentucky model (Equations A.2, A.3, A.5, A.7, A.9, A.10, A.15, A.16, A.18, A.19, and A.20)

Outflow of sediment from segment 2 (mass loading)
Inflow of sediment to segment 3 (mass loading)

| Segment width |

| Hydrologic input – Hydrograph (flow rate per unit width) (L/m/s) |

Segment 3

Compute sediment trapping with University of Kentucky model (Equations A.2, A.3, A.5, A.7, A.9, A.10, A.15, A.16, A.18, A.19, and A.20)

Outflow of sediment from segment 3 (mass loading)
Inflow of sediment to segment 4 (mass loading)

Continue to segment n
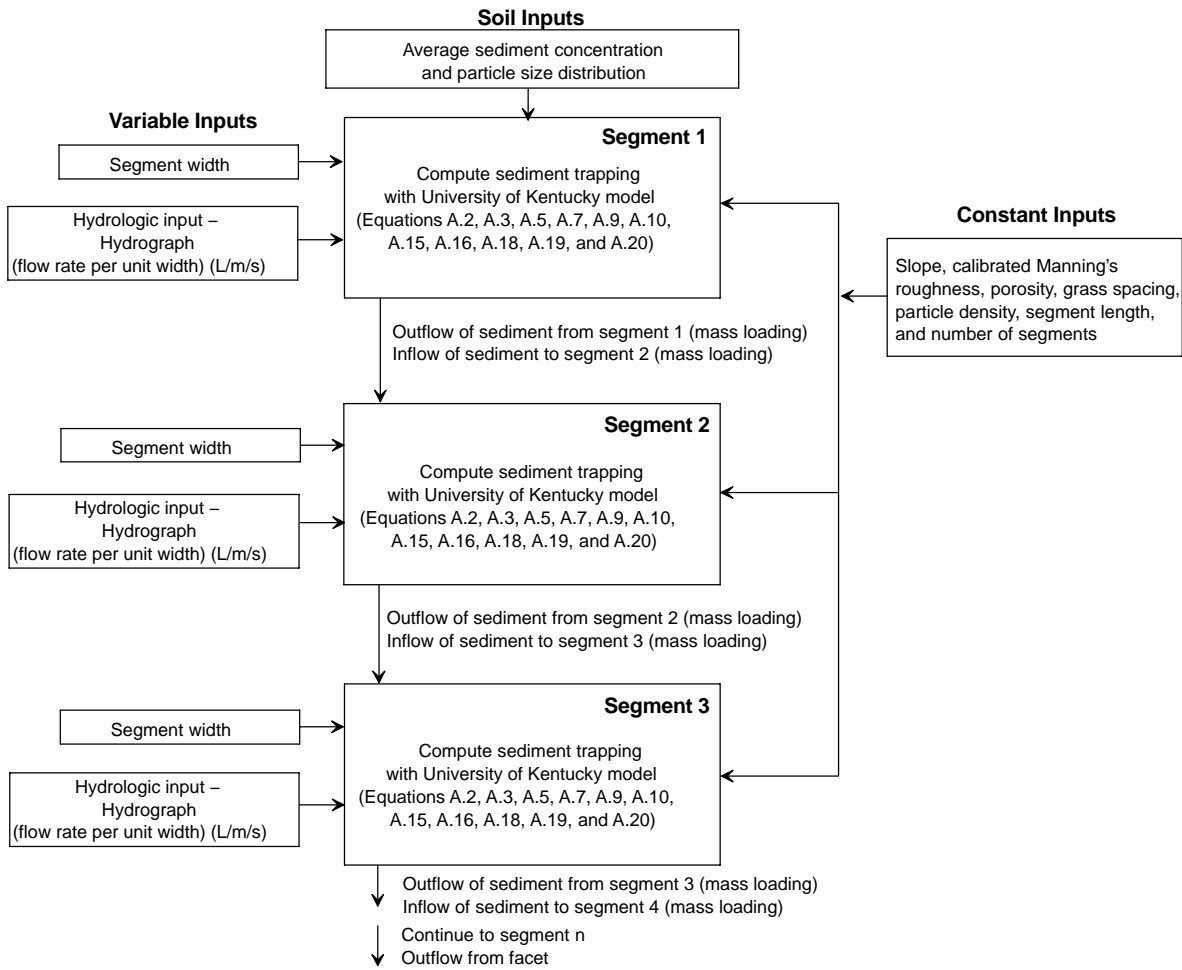Outflow from facet

Figure 3. Flowchart of segmental approach to sediment trapping in a vegetative filter using spreadsheet program.

It is assumed that medium-sized particles have a constant particle diameter of 0.012 mm, which is a diameter at the midpoint between 0.037 mm and 0.004 mm on a log scale (midpoint between coarse and fine particles). The fraction of sediment trapped in zone D for the coarse and medium particles is computed by equation A.19 for the individual segments and respective mean particle sizes. The program is setup to compute sediment trapping with and without the depth correction. When the depth correction is considered, the fraction of sediment trapped in zone D is adjusted according to equations A.15 and A.16. Equation A.18 is used to account for infiltration. The infiltration is estimated for each time step at each segment by comparing the water outflow from the previous segment to the water outflow from the present segment. As noted by Haan et al. (1994) and Inamdar (1993), fine particles (particles <0.004 mm) are not expected to be trapped by settling in zone D. However, the fine particles are trapped by infiltration according to equation A.18 using $T_{cs} = 0$. Once the trapping in a given segment is computed, the outflow of sediment is used as inflow for the next downstream segment.

To verify that the spreadsheet program accurately solves the equations of the model, results from the spreadsheet program were compared to other solutions. This process was termed code verification, based on the terminology of Shepherd and Geter (1995) and Refsgaard and Knudson (1996), where code verification involves comparison of the numerical solution generated by the code with one or more analytical solutions or with other numerical solutions. Verification ensures that the computer program accurately solves the equations that constitute the mathematical model.

The mixed particle size distribution component of the sediment filtration program was verified by comparing the results from the program to an example calculation of trapping efficiency using the University of Kentucky sediment filtration model from Haan et al. (1994). The parameters of the filter and sediment for this example are shown in table 1. The percent of sediment trapped as reported by Haan et al. (1994) is 68.1% versus a computed sediment trapping of 68.9% from the spreadsheet program (for no depth correction conditions). Thus, the results from the spreadsheet program

Table 1. Summary of parameters used for model verification.

Parameter	Haan et al. (1994)	VFSMOD Comparison
Inflow rate (L m^{-1} s^{-1})	6.87	1 and 4
Filter length (m)	15.24	12.95
Inflow sediment concentration (g L^{-1})	108.3	2
Fraction of incoming coarse sediment (particles >0.037 mm)	0.64	--
Fraction of incoming fine sediment (particles <0.004 mm)	0.18	--
Grass spacing (cm)	1.6	3.3
Slope	0.08	0.01
Calibrated Manning's roughness coefficient	0.056	0.05

compare well with the results from the example in Haan et al. (1994).

The program contains an alternative to the mixed particle size distribution by using the mean particle size (d_{50}) to characterize the sediment, as is done in VFSMOD. To further verify the model, results using this option were compared to results using VFSMOD. Two flow rate conditions were considered, both with no infiltration. The conditions considered are shown in table 1. For the 1 L m^{-1} s^{-1} peak flow rate conditions, the sediment trapping from VFSMOD was 95.1%, versus 95.9% from the spreadsheet program. For the 4 L m^{-1} s^{-1} peak flow rate condition, the sediment trapping reported by VFSMOD was 67.1%, versus 69.3% from the spreadsheet program. The results from the spreadsheet program for the mean particle size component compared well to the results from VFSMOD.

The modeling approach was applied to a specific field site, described below. The constant VF properties for this site are provided in table 2. The grass spacing is based on the average measured density of vegetation at the site. The calibrated Manning roughness coefficient is based on a tabular value from Haan et al. (1994) for a grass mixture.

Table 2. Summary of parameters in Clear Creek Buffer sediment filtration modeling.

Parameter	Value
Porosity of deposited sediment	0.50
Particle density (g cm^{-3})	2.65
Length of filter (m)	12.95
Segment length (m)	0.762
Grass spacing (m)	0.034
Slope (%), east grid	0.65
Slope (%), west grid	0.89
Calibrated Manning's roughness coefficient	0.050

STUDY SITE

SITE DESCRIPTION

Overland flow and sediment mass flow into and through a field-scale VF were monitored at the Clear Creek Buffer (see Helmers, 2003, for a detailed description of the study site and field experiments). The project site is located in Polk County in east-central Nebraska, and the VF was established in the spring of 1999. Vegetation in the filter consists of big bluestem (*Andropogon gerardii*), switchgrass (*Panicum virgatum*), and Indiangrass (*Sorghastrum nutans*). The area upstream of the VF is a furrow-irrigated field with furrow lengths of approximately 670 m and a crop row spacing of 0.762 m. The slope of the field is about 1%, and corn was grown in the field during the time period of this investigation. The field, including the filter, had been graded for furrow irrigation many years prior to this project. The furrows are perpendicular to the leading edge of the filter. The soil series in the location of the Clear Creek Buffer is a Hord silt loam (fine-silty, mixed, mesic Pachic Haplustolls) (USDA-SCS, 1974). Two 13 × 15 m grid areas in the Clear Creek Buffer were selected for investigation, with the 13 m dimension in the general direction of flow.

TOPOGRAPHY

Detailed topographic views of the two grid areas are shown in figures 4 and 5. In this research, these maps are termed the high-resolution topography. The contours on these topographic maps were developed with Surfer version 6.04 (Golden Software, 1997) using the kriging interpolation scheme. The location and elevation data (x,y,z coordinates) for these maps were obtained during the fall of 2001 using a total station (Nikon DTM-520) with measurement points on a 1.5 m grid in the 13 × 15 m area and on a 3 m grid outside the 13 × 15 m area.
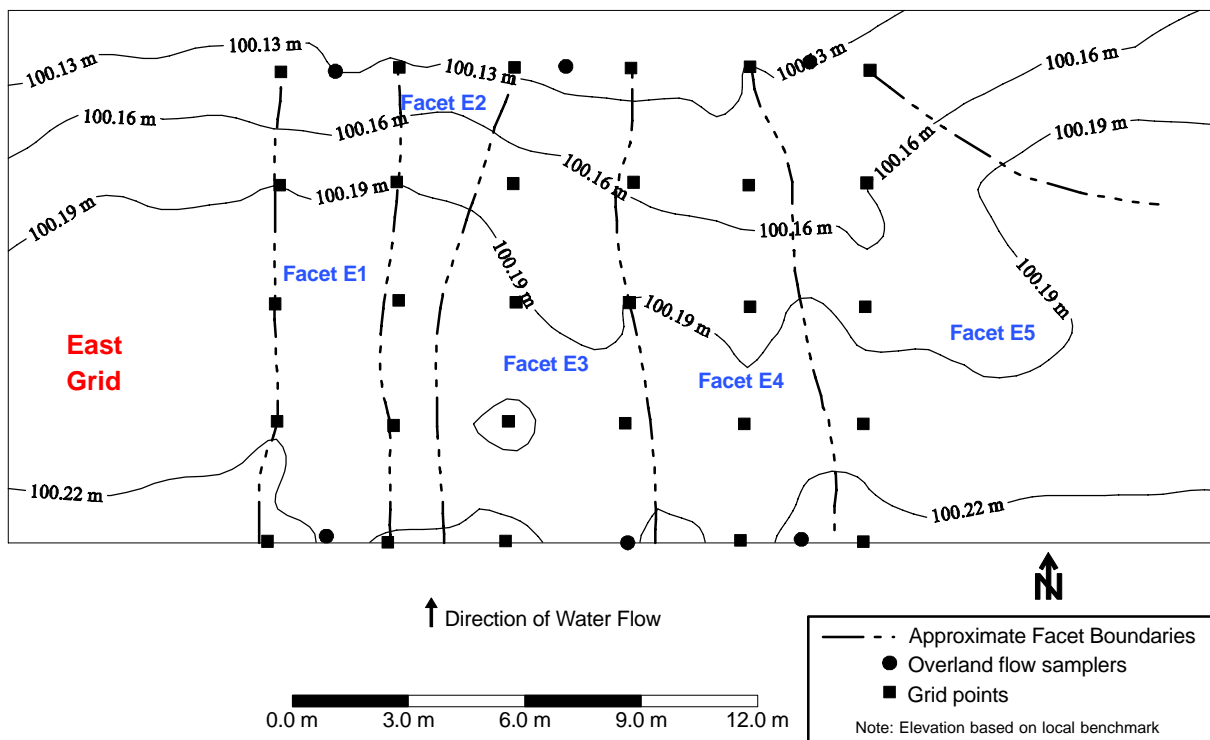

Figure 4. High-resolution topography of east grid with facet boundaries and locations of sampling equipment.
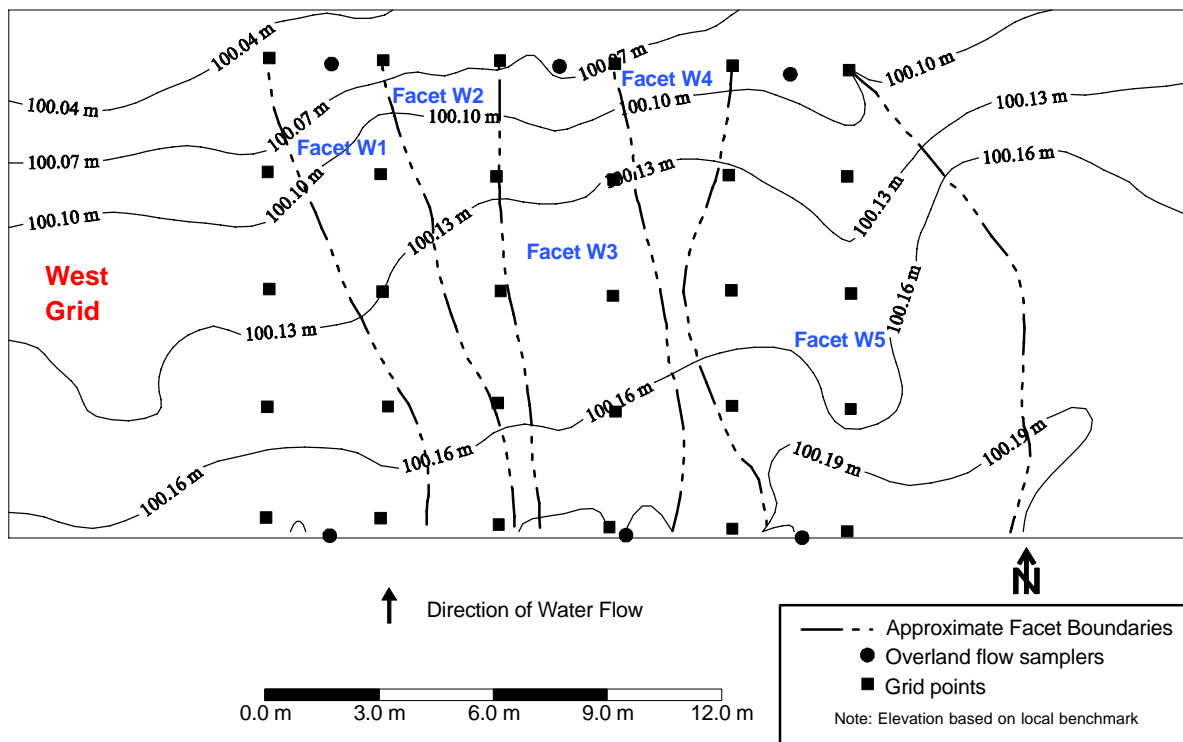
Figure 5. High-resolution topography of west grid with facet boundaries and locations of sampling equipment.

MONITORING EQUIPMENT

The locations of the overland flow samplers are shown in figures 4 and 5. The overland flow samplers, which sample a 0.3 m wide section, were developed during the course of this research project (Eisenhauer et al., 2002). A total of 12 overland flow samplers were installed at the Clear Creek Buffer, with six samplers in each grid area. Three samplers were installed at both the upstream and downstream edges of the filter. The samplers were used to obtain flow rate and water quality samples for estimating sediment loading to the VF.

In addition to the overland flow samplers, 60° V-notch trapezoidal flumes were installed approximately 30 m upstream from the filter in the irrigation furrows. At selected time intervals, the flow rate in the flumes was determined by manually recording the head. Water samples were collected at strategic times at each flume for estimating sediment loading to the VF. The suspended sediment concentration, herein called sediment, was based on the mass retained on a 1 μm filter. The retention rating for the filter was consistent with ASTM D3977, which states that a retention rating of <1.5 μm should be used for determining sediment concentration in water samples by filtration (ASTM, 2000).

RUNOFF EXPERIMENTS

The runoff from irrigation and natural rainfall-runoff events was monitored during the summers of 2001 and 2002. A total of five irrigation events (July 18, August 2, August 13, and August 23-24, 2001, and July 1, 2002) and one natural rainfall-runoff event (May 11, 2002) were monitored. The runoff was measured with both the flumes and the overland flow samplers for the irrigation events and with only the overland flow samplers for the natural rainfall-runoff event. The outflow was measured with the overland flow samplers at three points along the exit from each grid area. The inflow to the filter was measured using the three overland flow samplers in each grid area at the entrance to the filter and with multiple flumes positioned in the furrows. A summary of the runoff events at the Clear Creek Buffer is provided in table 3.

RESULTS AND DISCUSSION

The volumetric flow information is summarized in table 3. Many of the average inflow volumes for the measured events (4090 to 17,900 L m^{-1}) were in the range of the 1 h, 10-year return period precipitation event (11,000 L m^{-1}). However, the average peak flow rate for the events was

Table 3. Summary of runoff events at Clear Creek Buffer.

Runoff Event		Average Inflow Volume of Water (L m^{-1})	Average Peak Inflow Rate (L m^{-1} s^{-1})	Average Inflow Sediment Conc.[a] (g L^{-1})
Date	Location			
18 July 2001	East grid	17900	0.61	1.00
18 July 2001	West grid	7416	0.26	1.37
2 Aug. 2001	East grid	7120	0.40	0.15
2 Aug. 2001	West grid	4090	0.40	0.24
13 Aug. 2001	East grid	14389	0.48	0.23
13 Aug. 2001	West grid	7448	0.30	0.17
24 Aug. 2001	East grid	10397	1.27	0.94
23 Aug. 2001	West grid	12600	1.32	0.76
1 July 2002	East grid	9246	0.53	2.50
1 July 2002	West grid	12444	0.56	2.87
11 May 2002[b]	East grid	9587	1.06	1.27
11 May 2002[b]	West grid	8457	1.23	2.47

[a] "Sediment conc." refers to suspended sediment concentration.
[b] Natural rainfall-runoff event; all others are irrigation events.

below the peak flow rate for the 1 h, 10-year return period precipitation event. The estimated volumetric inflow per unit width for a 1 h duration, 10-year return period precipitation event (11,000 L m^{-1}) was calculated using the NRCS (SCS) curve number method. This assumed a 670 m field length contributing to the filter with a SCS runoff curve number of 75 and a field slope of 1.4%. The estimated peak flow rate for this 1 h duration, 10-year return period precipitation event was calculated using HEC-HMS (USCE, 1998). The calculated peak flow rates for the precipitation event described above were approximately 2.8, 2.1, and 1.75 L m^{-1} s^{-1} for a 670, 400, and 300 m contributing field length, respectively. These values are greater than the average peak inflow rates, which ranged from 0.26 to 1.29 L m^{-1} s^{-1}. In addition, using the Universal Soil Loss Equation (USLE) (Wischmeier and Smith, 1978) with a single-storm erosivity factor from Foster and Huggins (1977), an estimated erosion of 0.72 kg m^{-2} was computed. This relates to an average sediment concentration of approximately 44 g L^{-1} for the 11,000 L m^{-1} event described above.

Using the high-resolution topography (figs. 4 and 5), the contributing area to a downstream width of 3 m was determined by drawing orthogonal lines to the contours and proceeding upstream. Orthogonal lines to the contours give approximate flow lines, and the areas between adjacent flow lines are referred to as watershed facets (Bren, 1998). Figure 4 shows the facets for the east grid, and figure 5 shows the facets for the west grid. Facets E2 and W2 have the smallest contributing upstream width of the five facets, and facets E5 and W5 have the largest upstream contributing width. The full impacts of the contributing widths of facets E5 and W5 were not reflected in the irrigation events; because the edges of the irrigation sets corresponded to the edges of each grid area, inflow did not occur along the entire contributing width. The facets provide evidence that there are likely areas of converging and diverging overland flow in the VF. Further, the facets define the converging and diverging areas that were used in modeling.

The width of the facets varied within the VF (figs. 4 and 5). Facets E3 and W3 have a greater upstream width than downstream width, and facet W1 has a smaller upstream width than downstream width. These three facets were chosen for the modeling reported in this article. Using the width of each segment and the segment discretization of 0.762 m, the area of the three facets was computed (table 4). The area of each facet was compared to the potential area of the facet without flow convergence or divergence. This ratio is referred to as the convergence ratio (CR) and is defined as follows:

$$CR = 1 - \frac{FA_A}{FA_C} \quad (4)$$

where FA_A is the actual facet area, and FA_C is the facet area assuming constant width equal to upstream facet width.

Convergence ratios greater than zero indicate flow convergence, and facets with diverging flow have convergence ratios less than zero. The convergence ratios shown in table 4 reveal that facets W1 and W3 are overall diverging facets and facet E3 is a converging facet. Only facet E3 has both an upstream width greater than the downstream width and a convergence ratio greater than zero.

Table 4. Summary of segment width for watershed facets.

Segment	Width of Facet (m)		
	W1	W3	E3
1	2.3	3.5	5.4
2	2.2	3.8	5.45
3	2.2	3.9	5.5
4	2.2	3.9	5.5
5	2.2	3.9	5.5
6	2.15	3.85	5.4
7	2.15	3.8	5.25
8	2.3	3.9	5.1
9	2.4	4	4.8
10	2.55	4	4.6
11	2.8	3.9	4
12	3.05	3.6	3.6
13	3.05	3.6	3.45
14	3	3.5	3.4
15	3	3.3	3.4
16	3	3.15	3.25
17	3	3	3
Actual facet area (m^2)	33.19	47.70	58.37
Constant width area (m^2)	29.79	45.34	69.95
Convergence ratio	−0.11	−0.05	0.17

Sediment trapping in the Clear Creek Buffer was modeled using the sediment trapping spreadsheet program. Inputs to the program included sediment, vegetation, and filter characteristics and the water flow information generated from the MIKE SHE model. For the west grid, three different conditions were simulated: planar (CR = 0), non-planar in facet W1, and non-planar in facet W3. These two non-planar condition facets were simulated because, while both facets W1 and W3 were diverging facets based on their CR values, facet W1 had an upstream width less than its downstream width, and facet W3 had an upstream width greater than its downstream width. For the east grid, two different conditions were simulated: planar and non-planar in facet E3. The non-planar condition in facet E3 was simulated because this facet represented a converging facet with an upstream width greater than its downstream width and its CR was greater than zero.

Measured and modeled sediment trapping results for the west grid events are shown in table 5. The modeled sediment trapping for facet W1 (diverging facet) is greater than either the measured trapping or the planar condition sediment trapping. The diverging facet has a greater trapping efficiency than the planar condition probably because, in general, infiltration is higher. The quantity of infiltration is reflected by the infiltration ratios shown in table 5. Infiltration increases sediment trapping, partially because of convective removal of sediment-laden water by infiltration. In addition, there is a reduction of sediment transport capacity as water is removed from overland flow by infiltration. The results for the non-planar condition for facet W3 are similar to the results for the planar conditions. Even though the ratio of upstream to downstream width of facet W3 was 1.17, the area-based convergence ratio is slightly less than zero and as a result, it is understandable that the planar and non-planar conditions are similar for facet W3. It is interesting to note the similarity between the infiltration ratios of facet W3 and those for planar flow, which is understandable since the CR for facet W3 is close to zero (CR = −0.05) so the areas for planar flow and facet W3 are similar.

Table 5. Summary of sediment modeling for the west grid events at Clear Creek Buffer.

| | | Planar Conditions (CR = 0) | | Non-Planar Conditions | | | |
| | Average Measured Sediment Trapping[a] (%) | | | Facet W (CR = −0.11) | | Facet W3 (CR = −0.05) | |
Event		Modeled Sediment Trapping (%)	Infiltration Ratio[b]	Modeled Sediment Trapping (%)	Infiltration Ratio[b]	Modeled Sediment Trapping (%)	Infiltration Ratio[b]
18 July 2001	82	94	0.75	98	0.89	94	0.78
2 Aug. 2001	80	94	0.76	95	0.64	94	0.77
13 Aug. 2001	91	88	0.58	95	0.81	89	0.57
23 Aug. 2001	82	88	0.43	N.D.[c]	N.D.[c]	89	0.44
1 July 2002	79	82	0.41	92	0.72	83	0.47
11 May 2002	74	77	0.31	84	0.37	80	0.27

[a] Average measured sediment trapping based on average inflow of sediment and average outflow of sediment from the sampling equipment in the west grid.
[b] Infiltration ratio = volume infiltrated divided by inflow volume.
[c] N.D. = no data because of minimal flow in facet W1 for this event.

Analysis of variance was performed using SAS (2002) on the sediment trapping efficiency information shown in table 5, and contrasts were used to test treatment effects where the measured, planar conditions, non-planar conditions for facet W1 and the non-planar conditions for facet W3 were considered the treatment effects. The analysis of variance and results of the treatment contrasts are shown in table 6. There was a significant difference in the treatment means at the 0.05 significance level. From the individual contrasts, the measured and non-planar facet W1 conditions are significantly different. The measured and the non-planar facet W3 conditions were not significantly different at the 0.05 significance level. Both the non-planar facet W1 and facet W3 were diverging facets with convergence rations of −0.11 and −0.05, respectively, so it is understandable that the simulated sediment trapping efficiency would be greater for these conditions. The measured and the planar results are not significantly different at the 0.05 significance level. In addition, the planar results are not significantly different than the non-planar results. Since the planar and non-planar results are not significantly different, it is felt that the planar results for the west grid area are representative of the average conditions in the filter.

The results comparing the average measured sediment trapping and the modeled sediment trapping for the east grid are shown in table 7. Comparing the non-planar conditions for facet E3 versus the planar conditions reveals an insignificant reduction in sediment trapping using the non-planar conditions. While the ratio of upstream to downstream width was 1.8 for facet 3, the convergence ratio, based on area, was only 0.17. Thus, the level of convergence for facet 3 is not as great as might be expected and helps explain why there was no impact of convergence on sediment trapping. In addition, as before, the infiltration ratios of the planar and non-planar conditions are nearly identical, which

may explain why sediment trapping is essentially not affected by the flow convergence.

Analysis of variance was performed on the sediment trapping efficiency information from table 7, and contrasts were used to test treatment effects where the treatments were the measured, planar, and non-planar facet 3 conditions. The analysis of variance and results of the contrasts are shown in table 8. There was no significant difference in the measured and modeled results. Since the planar and non-planar results are not significantly different, the planar results are assumed to represent the average sediment trapping efficiency and sediment trapped for the east grid.

For the flow conditions and sediment loading measured at the Clear Creek Buffer, the converging flow areas (non-planar topographic conditions) had little impact on filter performance. This was probably because of the relatively low levels of convergence/divergence and possibly the relatively low inflow sediment concentration at the Clear Creek Buffer.

The average modeled sediment-trapping efficiency was within ±10% of the measured sediment trapping efficiency using planar conditions in 8 of the 12 cases (fig. 6). Again, the planar conditions relate to a convergence ratio of zero, so this is a case where we do not account for convergence or divergence. The modeled sediment trapped using the planar conditions was within ±10% of measured results in 7 of the 12 cases (fig. 7). In addition, there was greater than an order of magnitude difference in the amount of sediment trapped when comparing various events. To check the model's accuracy, the data were fit using linear regression to test if the

Table 6. Analysis of variance for sediment trapping efficiency for west grid events.

Source	df	Pr > F
Treatment (sediment trapping computation method)	3	0.0358
Contrast		
Measured versus planar		0.10
Measured versus non-planar facet W3		0.06
Measured versus non-planar facet W1		0.005
Planar versus non-planar facet W1		0.13
Planar versus non-planar facet W3		0.79
Non-planar facet W3 versus non-planar facet W1		0.20

Table 7. Summary of sediment modeling in facet 3 for the east grid events at Clear Creek Buffer.

| | | Planar Conditions | | Non-Planar Conditions Facet E3 / CR = 0.17 | |
Event	Average Measured Sediment Trapping (%)[a]	Modeled Sediment Trapping (%)	Infilt. Ratio[b]	Modeled Sediment Trapping (%)	Infilt. Ratio[b]
18 July 2001	74	83	0.45	83	0.44
2 Aug. 2001	92	89	0.64	88	0.59
13 Aug. 2001	85	85	0.48	84	0.46
24 Aug. 2001	93	90	0.51	90	0.49
1 July 2002	79	88	0.61	88	0.59
11 May 2002	83	81	0.42	83	0.43

[a] Average measured sediment trapping based on average inflow of sediment and average outflow of sediment from the sampling equipment in the east grid.
[b] Infiltration ratio = volume infiltrated divided by inflow volume.

Source	df	Pr > F
Treatment (sediment trapping computation method)	2	0.8062
Contrast		
Measured versus planar		0.58
Measured versus non-planar facet E3		0.58
Planar versus non-planar facet E3		1.0

slope of a regression line through the data was significantly different from one and to test if the intercept was significantly different from zero. From the linear regression, the slope was 1.17 and the intercept was −988 (fig. 7). Using a t-test, the intercept was not significantly different from zero at the 0.05 significance level, but the slope was significantly different from one at the 0.05 significance level. Based on the intercept not being significantly different from zero, the data were fit using linear regression holding the intercept equal to zero. For this case, the slope was computed to be 1.10, which was

found to not be significantly different from one at the 0.05 significance level. The coefficient of determination (R^2) for a 1:1 line was 0.83. Based on the slope not being significantly different from one, the measured and modeled sediment trapped compare reasonably. Considering that the modeled results are based on an uncalibrated model, the data validate the performance of the spreadsheet model for the conditions of the experiments. According to Refsgaard and Knudson (1996), validation is the process of demonstrating that a given site-specific model is capable of making accurate predictions for periods outside the calibration period. The spreadsheet model was not calibrated for the simulations that we conducted. Rather, the model's parameters were determined through field and laboratory experiments.

The greatest area-based convergence ratio for this investigation at the Clear Creek Buffer was only 0.17, but in many field conditions the ratio can be much greater. Dosskey et al. (2002) reported that the effective buffer area averaged 6%, 12%, 40%, and 80% of the gross buffer area (convergence ra-
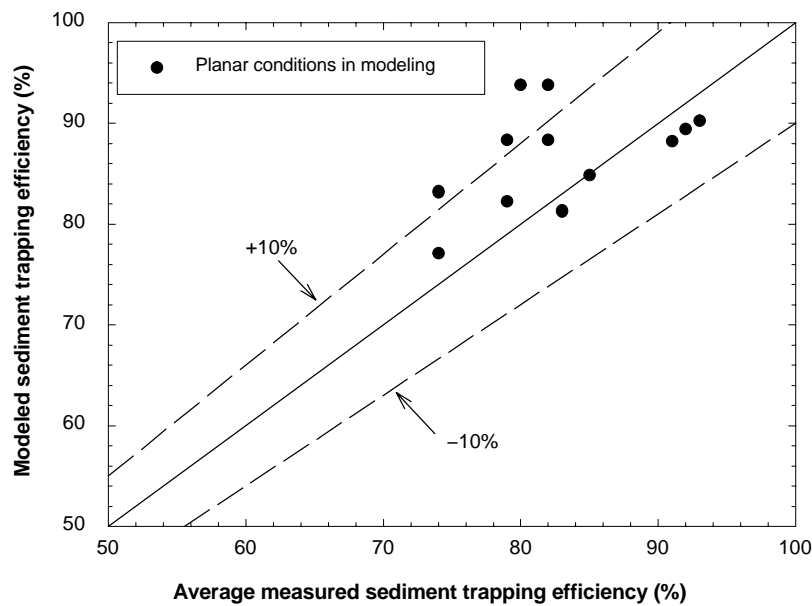

Figure 6. Measured versus modeled sediment trapping efficiency for all events.
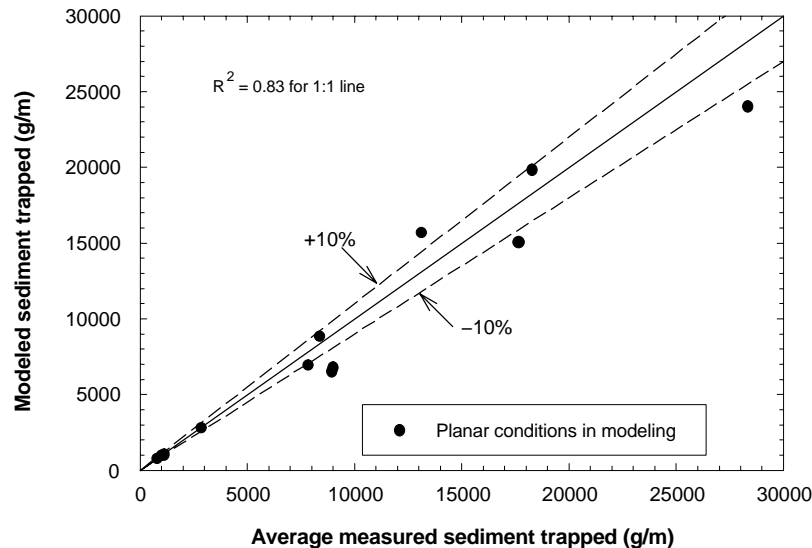

Figure 7. Measured versus modeled sediment trapped for all events.

tios of 0.94, 0.88, 0.60, and 0.20, respectively) for four farms in eastern Nebraska. Some of the convergence reflected in the convergence ratios in their study occurred within the field before the flow reached the filter.

To further investigate the effect of convergence on sediment trapping in a VF, model simulations were performed over a wider range of convergence ratios than measured in the Clear Creek Buffer. The ratios used were −0.35, −0.17, 0, 0.22, 0.3, 0.43, and 0.74. These values were chosen to get a broad range of convergence ratios. In these simulations, the flow convergence and divergence were artificially accomplished by narrowing or widening the segment width incrementally from upstream to downstream in the filter. A filter length of 13 m in the primary direction of flow was used, along with a standard runoff event with an inflow sediment concentration of 24 g L^{-1} and peak flow rate of 1.27 L m^{-1} s^{-1} (flow equal to the August 24, 2001, event). This inflow sediment concentration was used to simulate greater sediment loading than measured at the Clear Creek

Buffer. Two additional peak flow rates were used in the simulations: one at double the standard flow rate, and one at half the standard flow rate. Again, the August 24, 2001, event with a peak flow of 1.27 L m^{-1} s^{-1} was used as the standard.

The modeled sediment trapping efficiency and percent change in trapping efficiency are inversely related to convergence ratio (fig. 8), and as flow rate increases, sediment trapping efficiency decreases. For example, for the standard flow, the sediment trapping efficiency is 80% at zero convergence and 62% with a CR of 0.74. Further, with zero convergence, the trapping efficiency is about 62% for double flow, compared to 80% for the standard flow and 86% for half flow. In addition, at greater flow rates, the sediment trapping efficiency is more sensitive to convergence ratio. This is evident by the steepness of the lines in figure 8b. The double flow line is, in general, steeper than the standard and half flow lines. Convergence of overland flow negatively impacts filter performance, but diverging flow can positively impact filter
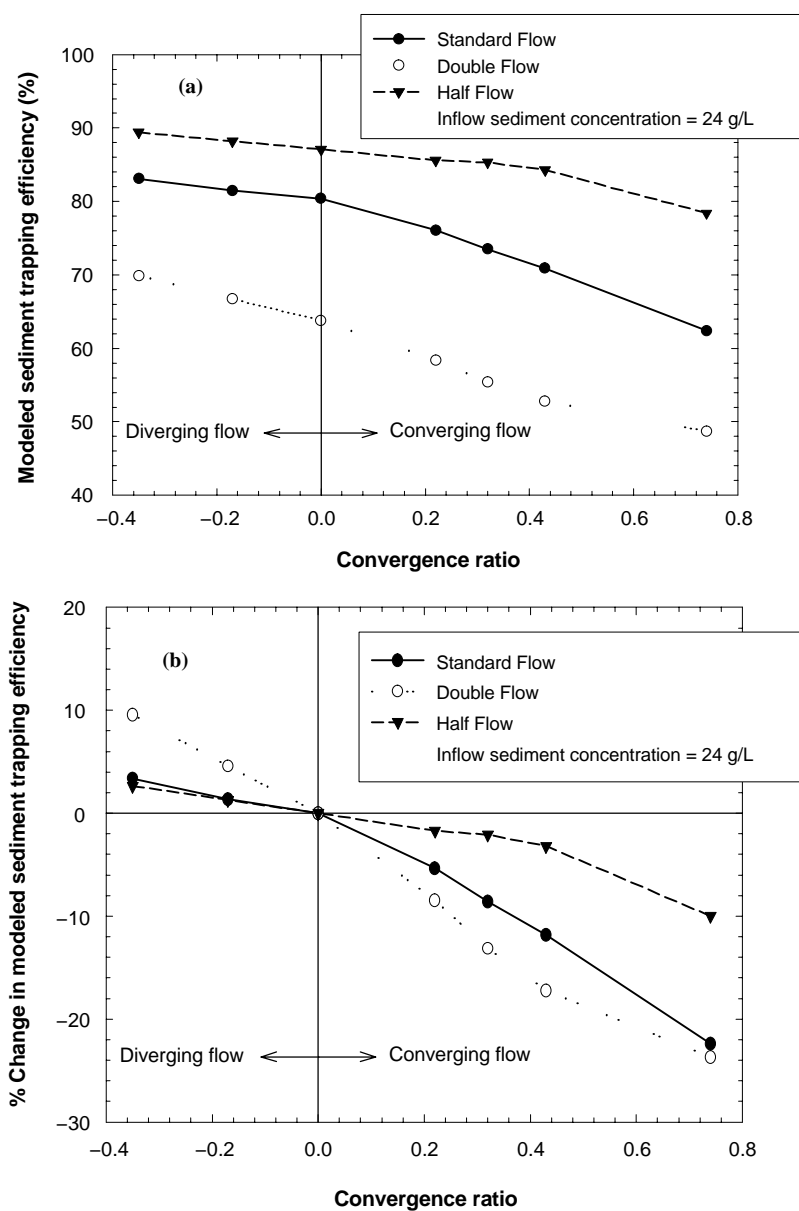

Figure 8. Sediment trapping efficiency as a function of convergence ratio for three water inflow rates: (a) modeled sediment trapping efficiency, and (b) % change in modeled sediment trapping efficiency.

Flow Event	Sediment Trapping Efficiency (%)		
	Planar	Convergence/Divergence Combination	
	CR = 0	CR = 0.22 and −0.17	CR = 0.31 and −0.35
Half standard flow event	87	87	87
Standard flow event (24 Aug. 2001 event)	80	78	77
Double standard flow event	64	62	61

[a] The combined effect of having a converging facet and a diverging facet
adjacent to one another.

performance. Trapping efficiency increased from 80% at
CR = 0 to about 84% at CR = −0.35.

In VF where convergence occurs, there could be corre-
sponding areas of divergence of overland flow. The inte-
grated or combined response of a converging facet next to a
diverging facet was reviewed using the data from figure 8.
The results for adjacent facets with convergence ratios of
0.22 and −0.17 and with convergence ratios of 0.31 and −0.35
were compared to a convergence ratio of zero (table 9). The
sediment trapping efficiency is based on the overall inflow
and outflow of sediment from the two facets combined. The
integrated effect of these converging and diverging facets
adjacent to one another had no impact at the half flow rate;
when compared to planar flow (CR = 0), there was a slight
reduction in sediment trapping in the filter at the standard and
double flow rates.

The effect of convergence ratio at various filter lengths
was also investigated using the standard runoff event. Filter
lengths of 6, 9, and 13 m were used in the simulations, with
a maximum convergence ratio of 0.43. As filter length
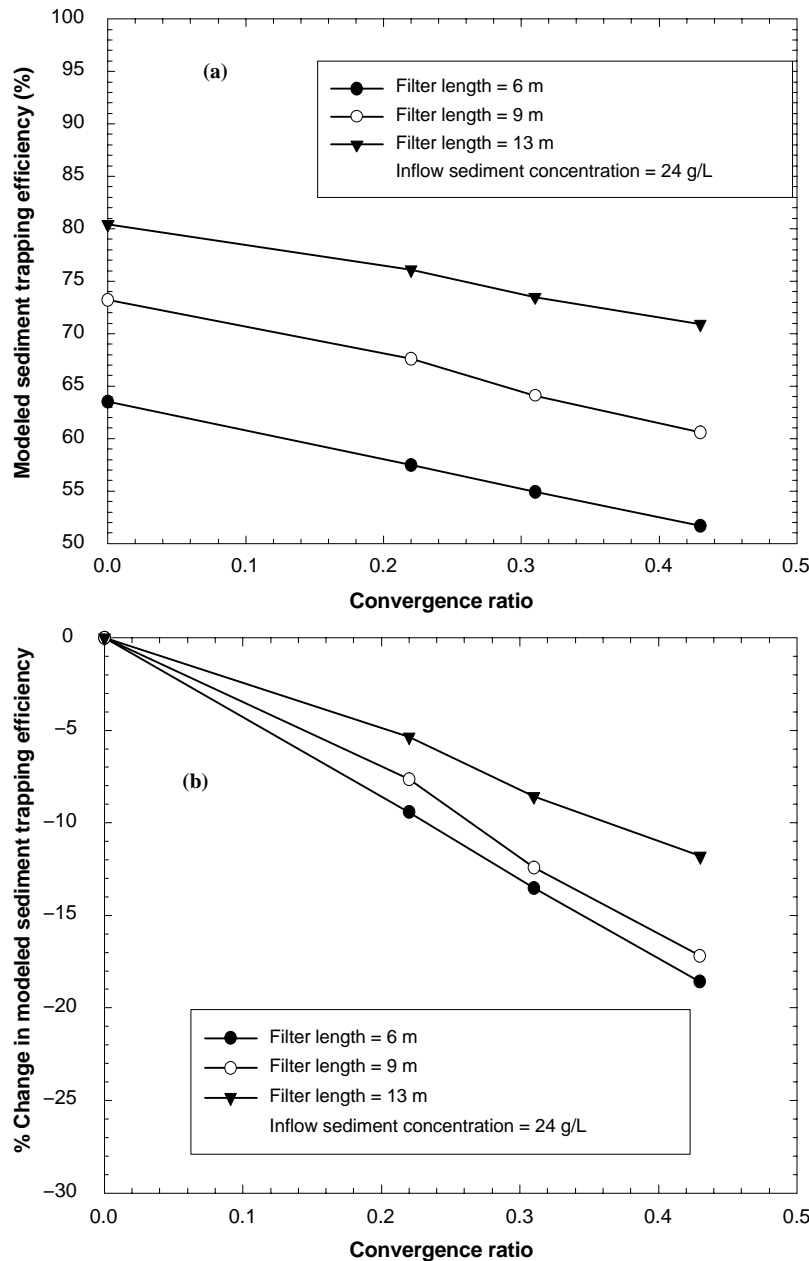decreases, the trapping efficiency decreases (fig. 9a). With no

**Figure 9. Sediment trapping efficiency as a function of convergence ratio for various filter lengths: (a) modeled sediment trapping efficiency, and (b) %
change in modeled sediment trapping efficiency (24 August 2001 inflow rate information).**

convergence, the trapping efficiency dropped from 80% for the 13 m filter to 73% for the 9 m filter and to 63% for the 6 m filter. At a convergence ratio of 0.43, the corresponding trapping efficiencies were 71%, 61%, and 52%, respectively. The trapping efficiency is more sensitive to convergence ratio for the shorter filter length since the absolute value in the percent change in the trapping efficiency is greater for the shorter filter lengths (fig. 9b).

In addition to convergence occurring within a VF (in-filter), convergence may occur prior to entering the VF, which is herein termed in-field convergence. In-field convergence was investigated using model simulations of the standard flow event and a filter length of 13 m. For the in-field convergence case, the flow was simulated to occur in a uniform width (direction perpendicular to primary flow direction) that was smaller in comparison to the full width of the field and filter. The convergence ratio is based on the reduced filter area and the filter area with the full filter width. The in-filter convergence used for comparison is the same as shown in figure 8a for the standard flow event.

Simulations were performed for in-field convergence ratios up to 0.73 (fig. 10). There was a difference between the two convergence scenarios at greater convergence ratios. In-field convergence resulted in a lower sediment trapping efficiency than in-filter convergence at CR greater than 0.30. For example, with CR = 0.70, in-filter convergence reduced the sediment trapping efficiency from 80% for the planar flow condition to 64% for the converging flow condition, while in-field convergence reduced trapping efficiency to 57%. For convergence in the field, the flow rate per unit of width at the entrance to the filter increases, and this increased flow velocity likely negatively impacts sediment trapping, especially in the upstream portion of the filter. From these results, it is clear that the location of convergence (in-field or in-filter) influences the degree of impact caused by convergence.

In field settings, in-field and in-filter convergence can occur simultaneously. While this scenario was not specifically investigated, the impact can be inferred by assuming double the standard flow conditions to be equivalent to having an in-field convergence ratio of 0.5. Double the standard flow conditions along with an in-filter convergence ratio of 0.5 had a sediment trapping efficiency of approximately 52% (fig. 8a). Thus, when assessing the impact of convergence on the performance of VF, in-field convergence, in-filter convergence, and their combined effects should be considered. In addition, there is a need for monitoring data that reflect these various convergence conditions. Collecting this information would be important for better understanding the processes that affect filter performance and testing the model approach discussed in this article over a broader range of convergence ratios.

CONCLUSIONS

Sediment trapping in a vegetative filter can be estimated using a modeling technique that incorporates a hydrology component (MIKE SHE), a sediment trapping component (University of Kentucky sediment filtration model), and a segmental model developed to predict the impact of converging and diverging flow. The two-dimensional modeling technique successfully predicted sediment trapping in a VF that had converging and diverging flow. Linear regression of the measured and modeled sediment trapped in a 13 m long filter revealed a slope not different from 1 and a R^2 of 0.83 for a 1:1 line. In 7 of the 12 cases, the model predicted sediment trapped within ±10% of measured data. The performance was considered quite good since the model was not calibrated.

While some convergence and divergence occurred at the Clear Creek Buffer, the non-planar flow had a negligible impact on sediment trapping. This is explained by the relatively low magnitude of the area based convergence ratios of the three facets that were studied. The convergence ratios ranged from −0.11 to 0.17. At these low-magnitude convergence ratios, the infiltration volume in the buffer was nearly equal for the planar and non-planar conditions. Because sediment trapping is influenced by infiltration, it makes sense that convergence has little effect on trapping if infiltration is not affected significantly.
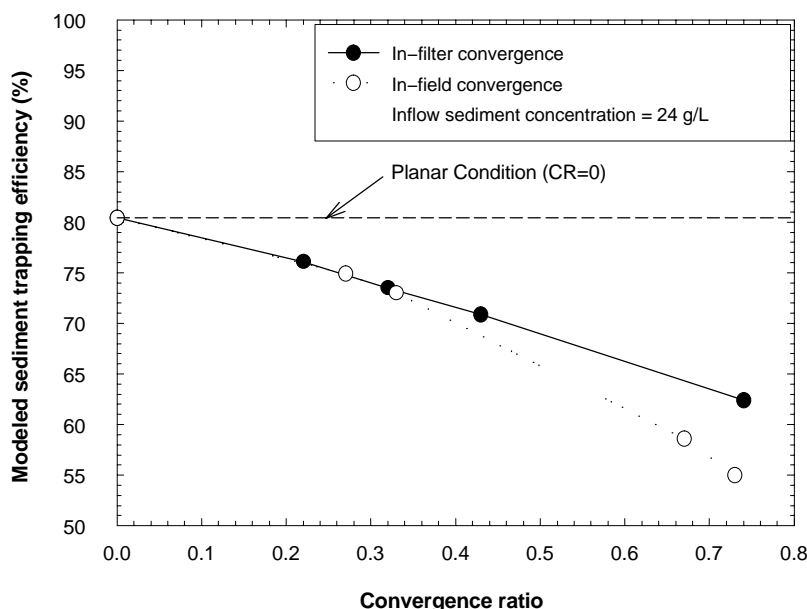

Figure 10. Sediment trapping efficiency as a function of convergence ratio (24 August 2001 inflow rate information).

Model simulations revealed that sediment trapping efficiency is reduced as convergence increases. For example, the sediment trapping efficiency was reduced from 80% for no convergence to 62% for a convergence ratio of 0.74. The impact of convergence on sediment trapping was greater at higher flow rates and at shorter filter lengths.

The location where the flow convergence occurs is also important. Both in-filter and in-field convergence were modeled. When the in-filter convergence ratio was 0.70, the sediment trapping efficiency dropped from 80% for the planar flow condition to 64% for the converging flow condition. When an equivalent in-field convergence occurred, the sediment trapping efficiency was reduced to 57%. The combined impact of having an in-field convergence ratio of 0.5 plus an in-filter convergence ratio of 0.5 resulted in a sediment trapping efficiency of 52%, compared to 80% for the no convergence case.

REFERENCES

ASTM. 2000. Standard test methods for determining sediment concentration in water samples. In *Annual Book of ASTM Standards*, vol. 11.02. D3977-97. West Conshohocken, Pa.: ASTM.

Barfield, B. J., E. W. Tollner, and J. C. Hayes. 1979. Filtration of sediment by simulated vegetation: I. Steady-state flow with homogeneous sediment. *Trans. ASAE* 22(5): 540-545.

Bren, L. J. 1998. The geometry of a constant buffer-loading design method for humid watersheds. *Forest Ecology and Management* 110: 113-115.

Daniels, R. B., and J. W. Gilliam. 1996. Sediment and chemical load reduction by grass and riparian filters. *SSSA J.* 60(1): 246-251.

Dillaha, T. A., R. B. Reneau, S. Mostaghimi, and D. Lee. 1989. Vegetative filter strips for agricultural nonpoint-source pollution control. *Trans. ASAE* 32(2): 513-519.

Dosskey, M. G., M. J. Helmers, D. E. Eisenhauer, T. G. Franti, and K. D. Hoagland. 2002. Assessment of concentrated flow through riparian buffers. *J. Soil and Water Conservation* 57(6): 336-343.

Einstein, H. A. 1942. Formula for the transportation of bed load. *Trans. ASCE* 107: 561-577.

Eisenhauer, D. E., M. J. Helmers, J. Brothers, M. G. Dosskey, T. G. Franti, A. Boldt, and B. Strahm. 2002. An overland flow sampler for use in vegetative filters. ASAE Meeting Paper No. 022050. St. Joseph, Mich.: ASAE.

Foster, G. R., and L. F. Huggins. 1977. Deposition of sediment by overland flow on concave slopes. In *Soil Erosion Prediction and Control*, 167-182. Special Publication No. 21. Ankeny, Iowa: Soil Conservation Society of America.

Golden Software. 1997. Surfer (Win 32). Version 6.04. Golden, Colo.: Golden Software, Inc.

Haan, C. T., B. J. Barfield, and J. C. Hayes. 1994. *Design Hydrology and Sedimentology for Small Catchments*. San Diego, Cal.: Academic Press.

Hayes, J. C., B. J. Barfield, and R. I. Barnhisel. 1979. Filtration of sediment by simulated vegetation: II. Unsteady flow with non-homogeneous sediment. *Trans. ASAE* 22(5): 1063-1067.

Hayes, J. C., B. J. Barfield, and R. I. Barnhisel. 1984. Performance of grass filters under laboratory and field conditions. *Trans. ASAE* 27(5): 1321-1331.

Helmers, M. J. 2003. Two-dimensional overland flow and sediment trapping in a vegetative filter. PhD diss. Lincoln, Neb.: University of Nebraska.

Inamdar, S. P. 1993. Modeling sediment transport in riparian vegetative filter strips. MS thesis. Lexington, Ky.: University of Kentucky.

Kutilek, M., and D. R. Nielson. 1994. *Soil Hydrology.* Cremlingen-Destedt, Germany: Catena Verlag.

Lowrance, R., L. S. Altier, R. G. Williams, S. P. Inamdar, J. M. Sheridan, D. D. Bosch, R. K. Hubbard, and D. L. Thomas. 2000. REMM: The Riparian Ecosystem Management Model. *J. Soil and Water Cons.* 55(1): 27-34.

Munoz-Carpena, R., J. E. Parsons, and J. W. Gilliam. 1999. Modeling hydrology and sediment transport in vegetative filter strips. *J. Hydrology* 214(1/4): 111-129.

Refsgaard, J. C., and B. Storm. 1995. "MIKE SHE." In *Computer Models of Watershed Hydrology*, 809-846. Water Resources Publication No. 5. V. P. Singh, ed. Highlands Ranch, Colo.: Water Resources Publications.

Refsgaard, J. C., and J. Knudson. 1996. Operational validation and intercomparison of different types of hydrological models. *Water Resources Research* 32(7): 2189-2202.

SAS. 2002. The SAS System for Windows. Ver. 8.02. Cary, N.C.: SAS Institute, Inc.

Schmitt, T. J., M. G. Dosskey, and K. D. Hoagland. 1999. Filter strip performance and processes for different vegetation, widths, and contaminants. *J. Environ. Quality* 28(5): 1479-1489.

Shepherd, R. G., and W. F. Geter. 1995. Verification, calibration, validation, simulation: Protocols in groundwater and AG/NPS modeling. In *Water Quality Modeling: Proc. International Symposium*, 87-90. C. Heatwole, ed. St. Joseph, Mich.: ASAE.

Sheridan, J. M., R. Lowrance, and D. D. Bosch. 1999. Management effects on runoff and sediment transport in riparian forest buffers. *Trans. ASAE* 42(1): 55-64.

Tollner, E. W., B. J. Barfield, C. T. Haan, and T. Y. Kao. 1976. Suspended sediment filtration capacity of simulated vegetation. *Trans. ASAE* 19(4): 678-682.

Tollner, E. W., B. J. Barfield, C. Vachirakornwatana, and C. T. Haan. 1977. Sediment deposition patterns in simulated grass filters. *Trans. ASAE* 20(5): 940-944.

Tollner, E. W., B. J. Barfield, and J. C. Hayes. 1982. Sedimentology of erect vegetal filters. *J. Hydraulics Div., ASCE* 108(12): 1518-1531.

USCE. 1998. HEC-HMS hydrologic modeling system. CPD-74. Washington, D.C.: U.S. Army Corps of Engineers.

USDA-SCS. 1974. Soil Survey of Polk County, Nebraska. Washington D.C.: U.S. Government Printing Office.

Wilson, B. N., B. J. Barfield, and R. C. Warner. 1982. A simulation model of the hydrology and sedimentology of surface mined lands: I. Modeling techniques. Special publication. Lexington, Ky.: University of Kentucky Department of Agricultural Engineering.

Wischmeier, D. A., and D. D. Smith. 1978. Predicting rainfall erosion losses: A guide to conservation planning. Agriculture Handbook No. 537. Washington D.C.: USDA.

APPENDIX

Table A.1. Summary of equations for University of Kentucky sediment filtration model.

Equation No.	Equation	Reference
A.1	$\tau_b = \rho g R_s S_c$	Tollner et al., 1982
A.2	$R_s = \dfrac{S_s d_f}{2d_f + S_s}$	Tollner et al., 1982
A.3	$V = \dfrac{1}{xn} R_s^{2/3} S_c^{1/2}$	Tollner et al., 1982
A.4	$q = V d_f$	Tollner et al., 1982
A.5	$\Psi = \dfrac{(\rho_s - \rho)}{\rho} \dfrac{d_p}{S_c R_s}$	Tollner et al., 1982
A.6	$\Phi_B^E = \dfrac{q_{sb}}{\rho_s} \left[\dfrac{\rho}{(\rho_s - \rho) g d_p^3} \right]^{1/2}$	Tollner et al., 1982
A.7	$\Phi_T^E = \dfrac{q_{st}}{\rho_s} \left[\dfrac{\rho}{(\rho_s - \rho) g d_p^3} \right]^{1/2}$	Tollner et al., 1982
A.8	$\Psi = 1.02(\Phi_B^E)^{-0.413}$	Tollner et al., 1982
A.9	$\Psi = 1.08(\Phi_T^E)^{-0.28}$	Tollner et al., 1982
A.10	$f = \dfrac{q_{si} - q_{sd}}{q_{si}}$	Haan et al., 1994
A.11	$q_{sba} = \dfrac{q_{si} + q_{sd}}{2}$	Haan et al., 1994
A.12	$T_S = \dfrac{q_{sd} - q_{so}}{q_{sd}} = \exp\left[-1.05 \times 10^{-3} (R_e)^{0.82} (N_f)^{-0.91} \right]$	Tollner et al., 1976
A.13	$R_e = \dfrac{V R_s}{v}$	Tollner et al., 1976
A.14	$N_f = \dfrac{V_s L(t)}{V d_f}$	Tollner et al., 1976
A.15	$C' = 0.5 \exp\left[-3 D_{ep} \right] + 0.5 \exp\left[15 \left(0.2 D_{ep} - D_{ep}^2 \right) \right]$	Wilson et al., 1982
A.16	$T_{cs} = C' T_s$	Wilson et al. 1982
A.17	$I = \dfrac{q_{wd} - q_{wo}}{q_{wd} + q_{wo}}$	Haan et al., 1994
A.18	$f_d = \dfrac{T_{cs} + 2I(1 - T_{cs})}{1 + I(1 - T_{cs})}$	Haan et al., 1994
A.19	$T_{si} = \exp\left[-1.05 \times 10^{-3} \left(\dfrac{V_n R_{sn}}{v} \right)^{0.82} \left(\dfrac{L_n V_s}{V_n d_{fn}} \right)^{-0.91} C_f \right]$	Inamdar, 1993
A.20	$C_f = \dfrac{n^{-0.91}}{m} \ln\left\{ 1 - \left[1 - \exp(m) \right]^{1/n} \right\}$	Inamdar, 1993

Table A.2. Nomenclature for equations A.1 through A.20.

Symbol	Definition
τ_b	The shear on the bed
ρ	Density of water
g	Acceleration of gravity
R_s	Hydraulic radius based on average spacing of media elements and the flow depth
S_c	Channel slope
S_s	Media spacing
d_f	Depth of flow
V	Mean flow velocity
xn	Calibrated Manning roughness coefficient
q	Volumetric water flow rate per unit width
Ψ	The shear intensity parameter
Φ_B^E	The Einstein bed load transport factor
Φ_T^E	The Einstein total sediment transport factor
ρ_s	The sediment density
d_p	Particle diameter
q_{sb}	The bed load transport rate per unit width
q_{st}	The total load transport rate per unit width
f	Fraction of the incoming coarse sediment deposited in the depositional wedge
q_{si}	Incoming sediment load rate
q_{sd}	Sediment transport rate downstream of the sediment wedge
q_{sba}	Average sediment load on the depositional wedge
T_s	Trapping efficiency in zone D(t)
q_{so}	Outgoing sediment load
R_e	Flow Reynolds number
N_f	Particle fall number
ν	Kinematic viscosity of the water-sediment mixture
V_s	Terminal settling velocity of the sediment particles
$L(t)$	Effective length of the filter
C'	Correction factor for zone D(t) trapping
T_{cs}	Corrected trapping efficiency in zone D(t)
D_{ep}	Average depth of sediment deposited in zone D(t)
I	Dimensionless term related to infiltration rate
q_{wd}	Flow rate at the inlet of zone D(t)
q_{wo}	Flow rate at the outlet of zone D(t)
f_d	Total fraction of sediment trapped in zone D(t)
T_{si}	Trapping efficiency of a segment
V_n	Mean flow velocity in segment
R_{sn}	Spacing hydraulic radius of segment
L_n	Length of segment
d_{fn}	Depth of flow in the segment
C_f	Correction factor
n	Number of segments
m	$= -0.00105(R_{et})^{0.82}(N_{ft})^{-0.91}$
R_{et}	Flow Reynolds number assuming flow properties in the segment apply to entire length of filter
N_{ft}	Particle fall number assuming flow properties in the segment apply to entire length of filter
D_{37}	Fraction of sediment finer than 0.037 mm after depositional wedge trapping
C_{f37}	Coarse fraction of sediment at entrance to filter
F	Fraction of incoming coarse sediment deposited in the depositional wedge
D_{ACW}	Average fraction finer for the coarse material after wedge deposition
D_{OCW}	Fraction finer on the original particle size distribution curve corresponding to fraction finer of coarse material after wedge deposition